Shuni Virus in Wildlife and Nonequine Domestic Animals, South Africa

Jumari Steyn, Pebetsi Motlou, Charmaine van Eeden, Marthi Pretorius, Voula I. Stivaktas, June Williams, Louwtjie P. Snyman, Peter E. Buss, Brianna Beechler, Anna Jolles, Eva Perez-Martin, Jan G. Myburgh, Johan Steyl, Marietjie Venter

We screened nonequine animals with unexplained neurologic signs or death in South Africa during 2010–2018 for Shuni virus (SHUV). SHUV was detected in 3.3% of wildlife, 1.1% of domestic, and 2.0% of avian species. Seropositivity was also demonstrated in wildlife. These results suggest a range of possible SHUV hosts in Africa.

Shuni virus (SHUV) (*Peribunyaviridae*: *Orthobunyavirus*) was isolated in the 1960s from livestock, *Culicoides* midges, and a febrile child in Nigeria (*1*,*2*). In South Africa, SHUV was identified as the causative agent of neurologic disease in horses (*3*); seropositivity was also demonstrated in 3.0% of veterinarians, suggesting human exposures (*4*). SHUV was subsequently identified in aborted livestock and cattle with neurologic disease in Israel, suggesting an extended range beyond Africa (*5*,*6*). We investigated other potential susceptible species in South Africa.

The Study

During February 2010–September 2018, a total of 101 whole blood, 71 serum, and 476 tissue specimens from 608 nonequine domestic animals, wildlife, and birds (19 fetuses, 118 juvenile and 471 adults) with unexplained neurologic or febrile disease or sudden unexplained death from across South Africa were submitted to the Zoonotic Arbo and Respiratory Virus Program, Centre for Viral Zoonoses, University of Pretoria (Pretoria, South Africa) as part of a passive zoonotic arbovirus surveillance program. We extracted RNA under Biosafety Level (BSL) 3 conditions using the QIAamp viral RNA mini kit (blood) or the RNeasy mini kit (tissue) (QIAGEN, https://www.qiagen.com), according to the manufacturer's recommendations. We screened all samples by a SHUV real-time reverse transcription PCR (rRT-PCR) (*7*) and a newly designed rRT-PCR targeting a conserved area of the S segment of the Simbu serogroup (Appendix, https://wwwnc.cdc.gov/EID/article/26/7/19-0770-App1.pdf). We confirmed PCR-positive samples by Sanger sequencing (Inqaba Biotech, https://www.inqababiotec.co.za) and phylogenetic analyses (Appendix). We also screened all specimens for West Nile (WNV), Wesselsbron (*8*), Middelburg (MIDV), Sindbis (*9*), and equine encephalosis viruses (*10*).

In addition, serum samples from African buffalo (*Syncerus caffer*) (n = 45) and white rhinoceros (*Ceratotherium simum*) (n = 48) from Kruger National Park were collected in March 2014 and June 2016, respectively, by South African National Parks and from wild Nile crocodiles (*Crocodylus niloticus*) (n = 34) from northern KwaZulu-Natal collected during 2009–2012 by the Faculty of Veterinary Sciences, University of Pretoria, as part of surveillance studies. We examined tissue samples from a SHUV PCR-confirmed positive buffalo (MVA43/10) microscopically under a light microscope using routinely prepared hematoxylin and eosin stained (*11*) histological sections at the Section of Pathology, Department of Paraclinical Sciences, Faculty of Veterinary Science, University of Pretoria. We subjected serum samples to an epitope-blocking ELISA (eb-ELISA) (*12*,*13*) with modifications to detect antibodies to SHUV (Appendix).

Author affiliations: University of Pretoria Faculty of Health, Pretoria, South Africa (J. Steyn, P. Motlou, C. van Eeden, M. Pretorius, V.I. Stivaktas, M. Venter); University of Pretoria Faculty of Veterinary Science, Pretoria (J. Williams, J.G. Myburgh, J. Steyl); Durban Natural Science Museum, Durban, South Africa (L.P. Snyman); South African National Parks, Kruger National Park, South Africa (P.E. Buss); Oregon State University, Corvallis, Oregon, USA (B. Beechler, A. Jolles); The Pirbright Institute, Woking, UK (E. Perez-Martin)

DOI: https://doi.org/10.3201/eid2607.190770

We calculated odds ratios (OR) and 95% CI in EpiInfo version 7.2.0.1 (https://www.cdc.gov/epiinfo/index.html). We excluded animals that were found dead, aborted, or stillborn from OR analysis.

We detected SHUV RNA in 15/608 (2.5%) animals tested from 10 different animal species: 12/361 (3.3%) wildlife, 2/196 (1.0%) nonequine domestic animals, and 1/51 avian species (2.0%) (Table 1). We detected SHUV in samples submitted from 2/62 (3.2%) white rhinoceroses, 2/50 (4.0%) sables, 1/15 (6.7%) warthog, 4/54 (7.4%) buffalo, 1/12 (8.3%) crocodiles, 1/5 (20.0%) giraffes, 1/4 (25.0%) springboks, 1/93 (1.1%) domestic bovids, and 1/10 (10.0%) alpacas (Table 1). We also detected SHUV in an exotic monal pheasant (1/13, 7.7%). Differential screening revealed co-infections with MIDV and WNV, suggesting that these arboviruses could co-circulate. A sable was also co-infected with *Theileria* sp. *sable* and *Theileria separate* (Table 1).

In 9/15 (60.0%, 95% CI 35.2%–84.8%) positive infections, we detected SHUV in the central nervous system (CNS) (Table 1), indicating passage across the blood–brain barrier, which suggests SHUV as the likely causal agent of the observed neurologic signs. This finding suggests that SHUV is not just an agent of subclinical infections or reproductive problems, such as abortion, as previously reported (*5*,*14*), but is also the likely etiology for neurologic disease in these species, as previously described for horses (*3*) and cattle (*6*). We did not detect SHUV RNA in aborted (n = 24) or stillborn (n = 16) animals. Eleven SHUV-positive animals showed neurologic signs (OR 1.8, 95% CI 0.2–14.4), with 2 animals also reported to be pyrexic (OR 2.0, 95% CI 0.4–9.4) or showing respiratory signs (OR 1.0, 95% CI 0.2–4.8) (Table 2). Three SHUV-positive animals were found dead (OR 1.8, 95% CI 0.5–6.4) (Table 2). Specific neurologic signs associated with SHUV infection included hind limb paresis progressing to quadriparesis with normal mentation (OR 6.7, 95% CI 2.0–22.5) (Table 2).

Positivity of infection was highest in the North West (4/47, 8.5% of samples submitted from North West), followed by Limpopo Province (8/132, 6.1%) (Table 1; Appendix Figure 1). SHUV was detected only in 2010 (4/15, 26.7%), 2017 (2/15, 13.3%), and 2018 (9/15, 60.0%) despite continuous surveillance throughout the years, suggesting that outbreaks may be sporadic rather than annual. SHUV PCR positives were detected during April–September in each of the 3 years (Appendix Figure 2).

Necropsy examination on the buffalo showed no specific macroscopic lesions on histopathology examination of brain tissue (Figure 1). Pathological changes that could be detected in regions of the brain

Table 1. Animals that tested positive for Shuni virus by real-time reverse transcription PCR, South Africa, 2010–2018*

Animal type	ID	No. positive/ no. tested	% Positive (95% CI)	Province where submitted	Positive specimen	Clinical signs	Co-infection
Domestic bovid	ZRU116/18	1/93	1.1 (0.0–3.1)	North West	Spleen	SUD	
White rhinoceros (*Ceratotherium simum*)	MVA11/10 ZRU137/18	2/62	3.2 (0.0–7.6)	Limpopo Free State	CNS	Neurologic	MIDV
Sable (*Hippotragus niger*)	ZRU419/17 ZRU121/18	2/50	4.0 (0.0–9.4)	North West Limpopo	Spleen	Hemorrhagic	Theileriosis
Warthog *(Phaecocherus africanus)*	MVA35/10	1/15	6.7 (0.0–19.3)	Limpopo	CNS	Neurologic, respiratory	
Buffalo (*Syncerus caffra*)	MVA43/10	4/54	7.4 (0.4–14.4)	Limpopo	CNS, whole blood	Neurologic, respiratory	
	ZRU77/18 ZRU97/18 ZRU166/18			Limpopo Limpopo Limpopo			
Monal (*Lophophorus impejanus*)	ZRU119/18	1/13	7.8 (0.0–22.2)	North West	CNS	SUD	
Crocodile (*Crocodylus niloticus*)	MVA08/10	1/12	8.3 (0.0–24.0)	Limpopo	CNS	Neurologic	
Alpaca (*Vicugna pacos*)	ZRU172/18	1/10	10.0 (0.0–28–6)	Western Cape	CNS	Neurologic, respiratory	
Giraffe (*Giraffa camelopardalis*)	ZRU87/18	1/5	20 (0.0–55.0)	North West	Whole blood	SUD	WNV
Springbok (*Antidorcus marsupialis*)†	ZRU261/17/3	1/4	25.0 (0.0–67.4)	Gauteng	Spleen	Neurologic	
Wildlife		12/361	3.3 (1.5–5.1)				
Domestic animals		2/196	1.1 (0.0–2.5)				
Avian		1/51	2.0 (0.0–5.8)				
Total		15/608	2.5 (1.2–3.7)				

*CNS, central nervous system; MIDV, Middelburg virus; SUD, sudden unexpected death; WNV, West Nile virus.
†Cluster with Sango virus.

Table 2. Clinical signs reported in wildlife, nonequine domestic animals, and birds upon submission to the Centre for Viral Zoonoses, South Africa, 2010–2018*

Sign	SHUV positive (%), n = 12	SHUV negative (%), n = 496	Odds ratio (95% CI)	p value†
Neurologic signs	11 (91.7)	415 (83.7)	1.8 (0.2–14.4)	0.9
Ataxia	2 (16.7)	102 (20.6)	0.8 (0.2–3.5)	1
Paralysis	3 (25.0)	61 (12.3)	2.3 (0.6–8.8)	0.4
Quadriparesis	8 (66.7)	112 (22.6)	6.7 (2.0–22.5)	<0.05
Recumbence	2 (16.7)	103 (20.8)	0.7 (0.2–3.4)	1
Pyrexia	2 (16.7)	44 (8.9)	2.0 (0.4–9.4)	0.7
Respiratory/dyspnea	2 (16.7)	79 (15.9)	1.0 (0.2–4.8)	1
Hemorrhage	1 (8.3)	10 (2.0)	4.3 (0.5–36.7)	0.6
Congenital deformities	0	7 (1.4)	Undefined	1

included mild white matter cerebro–cerebellar gliosis, especially microglial, associated with considerable glial apoptotic activity and occasional perivascular hemorrhage. In the spinal cord, occasional single neuronal necrosis (chromatolysis) and perineuronal hypereosinophilic bodies affecting the dorsal horns of the gray matter were distinctive. This finding seemed to be most severe in the lumbar spinal region. No evidence of demyelination or major immunological reaction was observed, apart from occasional perivascular lymphocytes. Development of appropriate antibodies for immunohistochemistry or probes for in situ hybridization may further describe the pathology of SHUV in animal tissue.

We used phylogenetic analyses on the small segment of the Simbu serogroup to verify the molecular results. All novel sequences from this study, with 1 exception, were closely related to SHUV strains identified in horses in South Africa (*3*) in clade 1a of lineage I within the Simbu serogroup (bootstopping:

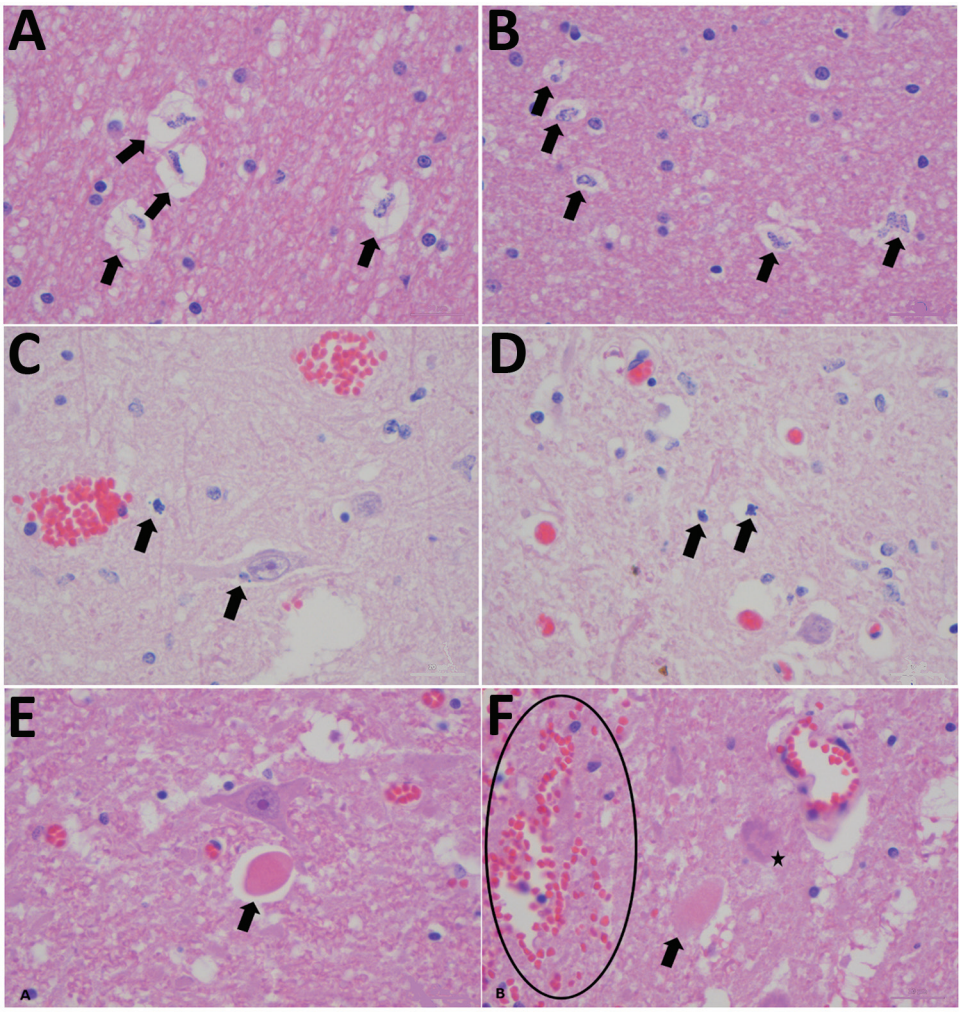

Figure 1. Histopathological changes in formalin-fixed brain tissue of a Shuni virus PCR-positive buffalo (MVA73/10) in South Africa that showed neurologic signs (original magnification 1000×). A, B) Cerebral white matter micro/astrogliosis and cytogenic edema (arrows). C, D) Glial (suspected oligodendroglia) apoptosis (arrows). E, F) Perineural hypereosinophilic bodies (arrows); perivascular and neuropil hemorrhage (circle); single-cell neuronal degeneration (chromatolysis) (star).

posterior probabilities = 89:0.99) (Figure 2). An isolate from a springbok (ZRU261_17_3) clustered with Sango virus (bootstopping: posterior probabilities = 67:0.94). P-distance analysis based on the partial small segment demonstrated few nucleotide differences between novel SHUV strains and reference strains (98.0%–100.0% identity). Wildlife specimens were submitted mostly from dead animals that were already undergoing postmortem cytolysis, inhibiting further genetic analysis and isolation of the virus. The use of a PCR designed to detect Simbu group/orthobunyavirus genus PCR rather than SHUV-specific PCR facilitated detection of these infections.

We detected antibodies to SHUV by an eb-ELISA in 3/44 (6.8%) African buffalo and 2/48 (4.2%) white rhinoceroses but none in crocodiles. SHUV-specific IgG was confirmed, using microtiter virus neutralization assay, in 1 buffalo and 1 rhinoceros. Two of 3 buffalo and 1 rhinoceros positive for SHUV epitope antibodies were negative by microtiter virus neutralization assay, suggesting that these antibodies may have been elicited in response to closely related orthobunyavirus. Confirmation for the third buffalo was not possible because of depleted serum.

Conclusion

Our findings suggest that SHUV may have a wide host range, including several wildlife and domestic species, and should be included in the differential diagnosis of neurologic disease in animals. This

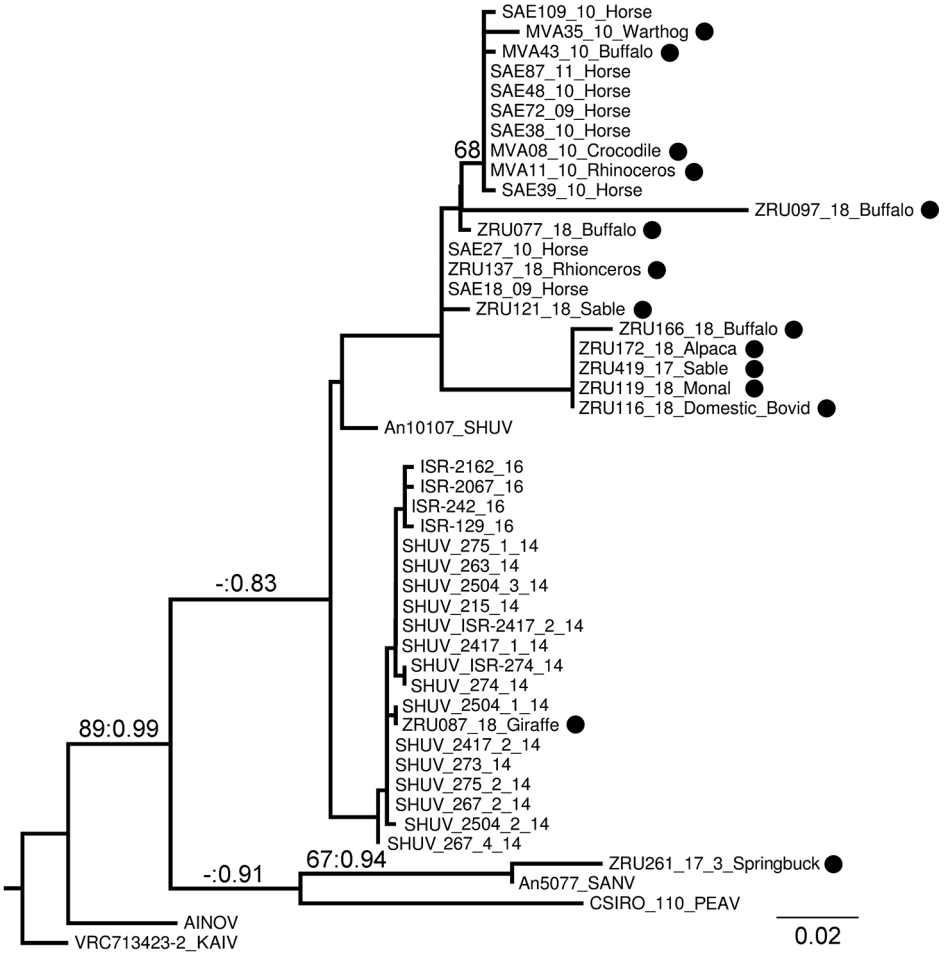

Figure 2. Phylogram of clade 1a, lineage I, of the Simbu serogroup (*15*) recovered from maximum-likelihood and Bayesian analyses of the small segment for SHUV isolates from wildlife and nonequine domestic animals, South Africa and reference sequences. Bootstrap values (maximum likelihood >60) and posterior probabilities (>0.8) are displayed on branches as support values. GenBank accession numbers for sequences from this study (black circles): MVA11_10_Rhinoceros, JQ726395; MVA08_10_Crocodile, JQ726396; MVA43_10_Buffalo, JQ726397; MVA35_10_Warthog, JQ726398; ZRU077_18_Buffalo, MK114084; ZRU121_18_Sable, MK114085; ZRU137_18_Rhinoceros, MK114086. GenBank accession numbers, virus types, and locations for reference sequences: An10107, AF362405, SHUV Nigeria; AINOV, M22011, Japan; VRC713423–2 KAIV, AF362394, India; SAE72_09_ Horse, HQ610138, South Africa; SAE27_10_Horse, HQ610139, South Africa; SAE38_10_Horse, HQ610140, South Africa; SAE39_10_Horse, HQ610141, South Africa; SAE48_10_Horse, HQ610142, South Africa; SAE109_10_Horse, HQ610143, South Africa; SAE18_09_Horse, KC510272, South Africa; SAE87_11_ Horse, KC525997, South Africa; Shuni_215_14, KP900859, Israel; Shuni_263_14, KP900860, Israel; Shuni_267_2_14, KP900861, Israel; Shuni_267_4_14, KP900862, Israel; Shuni_273_14, KP900865, Israel; Shuni_274_14, KP900867, Israel; Shuni_275_1_14, KP900869, Israel; Shuni_275_2_14, KP900871, Israel; Shuni_2417_1_14, KP900872, Israel; Shuni_2417_2_14, KP900875, Israel; Shuni_2504_1_14, KP900877, Israel; Shuni_2504_2_14, KP900878, Israel; Shuni_2504_3_14, KP900882, Israel; 2504_3_14, KU937313, Israel; SHUV_ISR-274_14, KT946779, Israel; SHUV_ISR-2417_2_14, KT946780, Israel; ISR-129_16, MF361846, Israel; ISR-242_16, MF361849, Israel; ISR-2067_16, MF361852, Israel; ISR-2162_16, MF361855, Israel; CSIRO 110, MH484320, Australia; An5077, AF362402, Nigeria. AINOV, ainovirus; KAIV, kaikalurvirus; PEAV, Peaton virus; SANV, Sango virus; SHUV, Shuni virus.

study highlights the role of this virus as a potential emerging zoonotic pathogen in Africa that warrants increased surveillance and further investigation. Future epidemiologic studies would benefit from an increased sample size and more extensive serosurveys. Investigation of human infections may define SHUV's importance as a zoonosis. The causative link between clinical manifestations in the various species and the evidence of SHUV infection must be regarded with caution because other possible infectious and noninfectious etiologies were not excluded by comprehensive investigations in all cases.

Acknowledgments

We thank participating veterinarians and veterinary pathologists from South Africa, as well as L.P. Snyman, for the help with the phylogenetic analyses.

This research was funded through the US CDC Global Disease Detection grant for Zoonotic arboviruses under grant no. 1U19GH000571-01-GDD Non-Research CoAg with the NHLS project 23 and UP Zoonotic Arbo and Respiratory virus program, 2012–2015, and by cooperative agreement no. 5 NU2GGH001874-02-00 with the University of Pretoria, 2015–2016. Buffalo samples were financed through BBSRC-USDA funding (grant no. BB/L011085/1) and transported under a Red Cross permit (LDK2016/9/1) to the BSL3 lab at CVZ. J. Steyn received doctoral scholarship form the NRF (grant no. 95175), the Meat Industry Trust (grant no. IT8114/98), the Poliomyelitis Research Foundation (grant no. 15/112).

This study was cleared by section 20 (12/11/1/1) approval through the Department of Agriculture Forestry and Fisheries (DAFF) (2014-October 2018) (M.V.) as well as by the animal ethics (H12-16) and section 20 (V057-15) (2017) of the University of Pretoria and the PhD research committee.

About the Author

Dr. Steyn is a virologist and PhD candidate at the Centre for Viral Zoonoses at the University of Pretoria, South Africa. Her primary research focuses on investigating arboviruses with zoonotic potential at human–animal interface areas.

References

1. Causey OR, Kemp GE, Causey CE, Lee VH. Isolations of Simbu-group viruses in Ibadan, Nigeria, 1964–69, including the new types Sango, Shamonda, Sabo and Shuni. Ann Trop Med Parasitol. 1972;66:357–62. https://doi.org/10.1080/00034983.1972.11686835
2. Lee VH. Isolation of viruses from field populations of *Culicoides* (Diptera: Ceratopogonidae) in Nigeria. J Med Entomol. 1979;16:76–9. https://doi.org/10.1093/jmedent/16.1.76
3. van Eeden C, Williams JH, Gerdes TGH, van Wilpe E, Viljoen A, Swanepoel R, et al. Shuni virus as cause of neurologic disease in horses. Emerg Infect Dis. 2012;18:318–21. https://doi.org/10.3201/eid1802.111403
4. van Eeden C, Swanepoel R, Venter M. Antibodies against West Nile and Shuni viruses in veterinarians, South Africa. Emerg Infect Dis. 2014;20:1409–11. https://doi.org/10.3201/eid2008.131724
5. Golender N, Brenner J, Valdman M, Khinich Y, Bumbarov V, Panshin A, et al. Malformations caused by Shuni virus in ruminants, Israel, 2014–2015. Emerg Infect Dis. 2015;21:2267–8. https://doi.org/10.3201/eid2112.150804
6. Golender N, Bumbarov V, Assis I, Beer M, Khinich Y, Koren O, Edery N, Eldar A, et al. Shuni virus in Israel: neurological disease and fatalities in cattle. Transbound Emerg Dis. 2019;66:1126–31. https://doi.org/10.1111/tbed.13167
7. Van Eeden C, Zaayman D, Venter M. A sensitive nested real-time RT-PCR for the detection of Shuni virus. J Virol Methods. 2014;195:100–5. https://doi.org/10.1016/j.jviromet.2013.10.008
8. Zaayman D, Human S, Venter M. A highly sensitive method for the detection and genotyping of West Nile virus by real-time PCR. J Virol Methods. 2009;157:155–60. https://doi.org/10.1016/j.jviromet.2008.12.014
9. van Niekerk S, Human S, Williams J, van Wilpe E, Pretorius M, Swanepoel R, et al. Sindbis and Middelburg old world alphaviruses associated with neurologic disease in horses, South Africa. Emerg Infect Dis. 2015;21:2225–9. https://doi.org/10.3201/eid2112.150132
10. van Niekerk M, Freeman M, Paweska JT, Howell PG, Guthrie AJ, Potgieter AC, et al. Variation in the NS3 gene and protein in South African isolates of bluetongue and equine encephalosis viruses. J Gen Virol. 2003;84:581–90. https://doi.org/10.1099/vir.0.18749-0
11. Bancroft JD, Gamble M, editors. Theory and practice of histological techniques. Edinburgh: Churchill Livingstone; 2002.
12. Blitvich BJ, Marlenee NL, Hall RA, Calisher CH, Bowen RA, Roehrig JT, et al. Epitope-blocking enzyme-linked immunosorbent assays for the detection of serum antibodies to West Nile virus in multiple avian species. J Clin Microbiol. 2003a;41:1041–7. https://doi.org/10.1128/JCM.41.3.1041-1047.2003
13. Blitvich BJ, Bowen RA, Marlenee NL, Hall RA, Bunning ML, Beaty BJ. Epitope-blocking enzyme-linked immunosorbent assays for detection of West Nile virus antibodies in domestic mammals. J Clin Microbiol. 2003b;41:2676–9. https://doi.org/10.1128/JCM.41.6.2676-2679.2003
14. Mathew C, Klevar S, Elbers ARW, van der Poel WHM, Kirkland PD, Godfroid J, et al. Detection of serum neutralizing antibodies to Simbu sero-group viruses in cattle in Tanzania. BMC Vet Res. 2015;11:208. https://doi.org/10.1186/s12917-015-0526-2
15. Saeed MF, Li L, Wang H, Weaver SC, Barrett ADT. Phylogeny of the Simbu serogroup of the genus *Bunyavirus*. J Gen Virol. 2001;82:2173–81. https://doi.org/10.1099/0022-1317-82-9-2173.

Address for correspondence: Marietjie Venter, Zoonotic Arbo and Respiratory Virus Program, Centre for Viral Zoonoses, Department of Medical Virology, University of Pretoria, Pretoria, South Africa; email: marietjie.venter@up.ac.za

Article DOI: https://doi.org/10.3201/eid2607.190770

Shuni Virus in Wildlife and Nonequine Domestic Animals, South Africa

Appendix

Methods and Validations

We designed and validated a new small (S) segment real-time reverse transcription PCR (rRT-PCR) assay using a more conserved region of the S segment of the Simbu virus serogroup, situated between genomic positions 152–304 (152 base pair [bp]) of SHUV sequence KC510272. We designed a group-specific primer set using viruses in the Simbu virus serogroup (Ortho(SimbuF152): $5'^{152}$TAGAGTCTTCTTCCTCAAYCAGAAGAAGGCC$'3^{184}$ and Ortho(SimbuR304): $5'^{276}$GTYAMGGCAMTGTCTGGCACAGGATTTG$'3^{304}$)) and a TaqMan probe (Ortho(Simbu-probe252)($5'^{252}$TGGTTAATAACCATTTTCC$'3^{270}$)) including the available SHUV strains. For the Simbu/orthobunyavirus-specific RT-PCR assay, a 50 μL reaction consisted of AgPath-ID 2x RT-PCR buffer (ThermoFisher Scientific, https://www.thermofisher.com), 10 μL RNA, 400 nM of the forward and reverse primers, 150 nM of the TaqMan probe, and a 25x RT-PCR Enzyme Mix (ThermoFisher Scientific). The 1-step real-time RT-PCR was performed on a ViiA 7 Real-Time PCR System (Applied Biosystems, https://www.thermofisher.com) with cycling conditions of 50°C for 30 min, 94°C for 2 min, and 45 cycles of 94°C for 15 sec and 58°C for 1 min. To validate the rtRT-PCR, a dilution series of RNA isolated from a culture control of SHUV strain SAE18/09 were created; the new Simbu/orthobunyavirus rRT-PCR ran in triplicate in parallel with the published SHUV-specific rRT-PCR (*1*). The published PCR could be detected up to 10^{-4} by melting curve analysis and up to 10^{-6} on an agarose gel. Each dilution could be detected by the Simbu/orthobunyavirus rRT-PCR at cycle threshold (Ct) values of 20 to 40 in triplicate up to 10^{-5} and with 2/3 replicates detected at 10^{-6} by the rRT-PCR at Ct values of 40 and visible on an agarose gel with the expected band sizes of 152 base pairs up to 10^{-6} (Appendix Table and Appendix Figure 3). Archived SHUV-positive clinical specimens were amplified in parallel with the SHUV-specific rRT-PCR (*1*) and the new Simbu/orthobunyavirus rtRT-PCR with amplification of 4/12 (33.3%)

samples with the SHUV specific rRT-PCR compared to 8/12 (66.7%) samples amplifying with the new Simbu/orthobunyavirus rtRT-PCR. This is likely the result of RNA degradation in the archived specimens with the new PCR being able to detect shorter fragments than the original PCR. Of a blinded panel of archived SHUV strains that could be detected with the SHUV nested rtRT-PCR (1), all could be detected by the Simbu/orthobunyavirus rRT-PCR, whereas no other arboviruses (WNV, MIDV, Sindbis, or Wesselsbron virus) could be detected. Three SHUV strains that could not be detected by the SHUV-specific PCR (*1*) was also detected in horses (reported elsewhere).

We edited and analyzed sequencing data using CLC Main Workbench 8 (https://www.qiagenbioinformatics.com). Multiple sequence alignments were done using multiple alignment using fast Fourier transform (MAFFT), v7 (http://mafft.cbrc.jp/alignment/server/index.html), and Mega 6.06 (Molecular Evolutionary Genetics Analysis software, https://www.megasoftware.net) was used to assemble concatenated sequences. Reference sequences from the Simbu serogroup were selected based on the gene segment and downloaded from GenBank. The best-fit model was estimated using jModelTest, v2.1.4 (https://github.com/ddarriba/jmodeltest2) and used to construct maximum likelihood trees using RAxML (https://cme.h-its.org/exelixis/web/software/raxml) with AutoMRE function. Bayesian analysis was performed in MrBayes version 3 (https://cme.h-its.org/exelixis/web/software/mrbayes). MrBayes 3 was used for Bayesian inference running 4 cold chains for 10,000,000 iterations, saving every 1000th tree. The bootstrap support of the maximum likelihood analysis for a concatenated (nucleotides [nt] = 490) phylogram of the “long” (nt = 338) (genomic position 305–643) and “short” (nt = 152) (genomic position 152–304) sequences was calculated from 650 replicates using the autoMRE bootstepping criterion in RaxML. GTR+G were applied to a partitioned dataset with bootstraps (bs) >60 viewed as supportive of the clustering (Figure 2). HKY+G and TIM2+G models were respectively applied to 2 unlinked partitions. All posterior probabilities (pb) >0.8 were viewed as strong support (Figure 2). Tracer v1.6 was employed for assessing distribution and effective sample size. Effective sample size (ESS) value was >>200. The number of nucleotide differences between sequences was determined using p-distance analysis with 1000 bootstrap replicates in MEGA 6.06. All SHUV nucleotide sequences >200 nt were submitted to GenBank prior to the study

(JQ726395–JQ726398 and MK114084–MK114086). Virus isolation was also attempted on positive tissue specimens, but it was not successful.

To perform the eb-ELISA, microtiter plates (CELLSTAR, Greiner Bio-One, Frickenhausen, Germany) were coated with 100 μL of a 1:100 dilution of SHUV-specific cell lysate antigen diluted in carbonate–bicarbonate buffer. SHUV antigen were produced using detergent basic buffer extraction of infected cell culture with reference strain SAE18/09 (*2*,*3*). Vero cells in 175 cm^2 flasks were infected and cultured until 80.0% cytopathic effects were observed. The cell suspension was clarified by centrifugation at 10,000 × *g* for 10 minutes at 4°C to pellet the cells. Cells were then washed in 0.01 M borate buffer saline (BBS) (Sigma-Aldrich, https://www.sigmaaldrich.com), pH 9.0. Cell pellet was resuspended in BBS and 10 μL 1.0% (vol/vol) Triton X-100 (Sigma-Aldrich). The suspension was sonicated for 10 minutes, placed on ice, and centrifuged at 10,000 × *g* for 5 min at 4°C, after which the supernatant was collected. Antigen coated plates were incubated overnight at 4°C in a humidity chamber. Two hundred microliters of blocking buffer (PBS containing 10.0% skim milk) was added to each well and incubated for 1 hour at 37°C. Test sera were diluted 1:4 in 2.0% skim milk and 100 μL was added. Plates were then incubated for 24 hours at 37°C. SHUV-specific hyperimmune mouse ascites fluid (MHIAF) polyclonal antibody (M12357A1, CDC, Fort Collins, USA) was diluted 1:200 in 2.0% skim milk and 100 μL was added to each well. Plates were then incubated for 1 hour at 37°C after which 100 μL of horseradish peroxidase (HRP)-conjugated rabbit anti-mouse IgG antibody (Bio-Rad Laboratories, https://www.bio-rad.com) was added at a dilution of 1:2000. Plates were incubated for 1 hour at 37°C. ABTS (2,2_azino-bis[3-ethylbenzthiazoline-6-sulfonic acid]) was added and plates were incubated for 30 minutes. After each incubation step, plates were washed 3 times with phosphate-buffered saline containing 0.05% Tween 20 (Sigma-Aldrich). The eb-ELISA was optimized using checkerboard titrations of different dilutions of the antigen and the antibody. Test sera were added at 1:4 dilution as recommended (*4*,*5*). The antibody binding was manually calculated, and expressed as percentage inhibition (PI) value, with a cutoff value of 40.0% PI. Positive reactions were confirmed with microtiter virus neutralization assay (micro-VNT) as described, using a 10^3 tissue-culture infective dose of SHUV culture (SAE18/09, passage 6) (*2*). A limitation to the validation of the eb-ELISA was the availability of known SHUV-positive animals other than horses. The eb-ELISA was therefore

optimized and validated using horse sera. Results of this study allows for further validation of the assay using wildlife sera.

References

1. van Eeden C, Zaayman D, Venter M. A sensitive nested real-time RT-PCR for the detection of Shuni virus. J Virol Methods. 2014;195:100–5.

2. van Eeden C, Swanepoel R, Venter M. Antibodies against West Nile and Shuni viruses in veterinarians, South Africa. Emerg Infect Dis. 2014;20:1409–11.

3. Ksiazek TG, West CP, Rollin PE, Jahrling PB, Peters CJ. ELISA for the detection of antibodies to Ebola viruses. J Infect Dis. 1999;179(Suppl 1):S192–8.

4. Blitvich BJ, Marlenee NL, Hall RA, Calisher CH, Bowen RA, Roehrig JT, et al. Epitope-blocking enzyme-linked immunosorbent assays for the detection of serum antibodies to West Nile virus in multiple avian species. J Clin Microbiol. 2003;41:1041–7.

5. Blitvich BJ, Bowen RA, Marlenee NL, Hall RA, Bunning ML, Beaty BJ. Epitope-blocking enzyme-linked immunosorbent assays for detection of West Nile virus antibodies in domestic mammals. J Clin Microbiol. 2003;41:2676–9.

Appendix Table. Summary of the TaqMan Simbu/orthubunyavirus genus specific real-time RT-PCR assay showing the cycle threshold values, mean, and standard deviation.

Dilution	Ct values (in triplicate)			Mean	Standard deviation
10^{0}	16.97	18.28	17.26	17.50	0.69
10^{-1}	20.96	20.94	20.82	20.91	0.08
10^{-2}	24.65	24.83	24.8	24.76	0.10
10^{-3}	28.54	28.58	28.65	28.59	0.56
10^{-4}	32.35	32.2	31.1	31.88	0.69
10^{-5}	36.57	36.17	36.21	36.32	0.22
10^{-6}	40.16	40.08	40.11	40.12	0.06

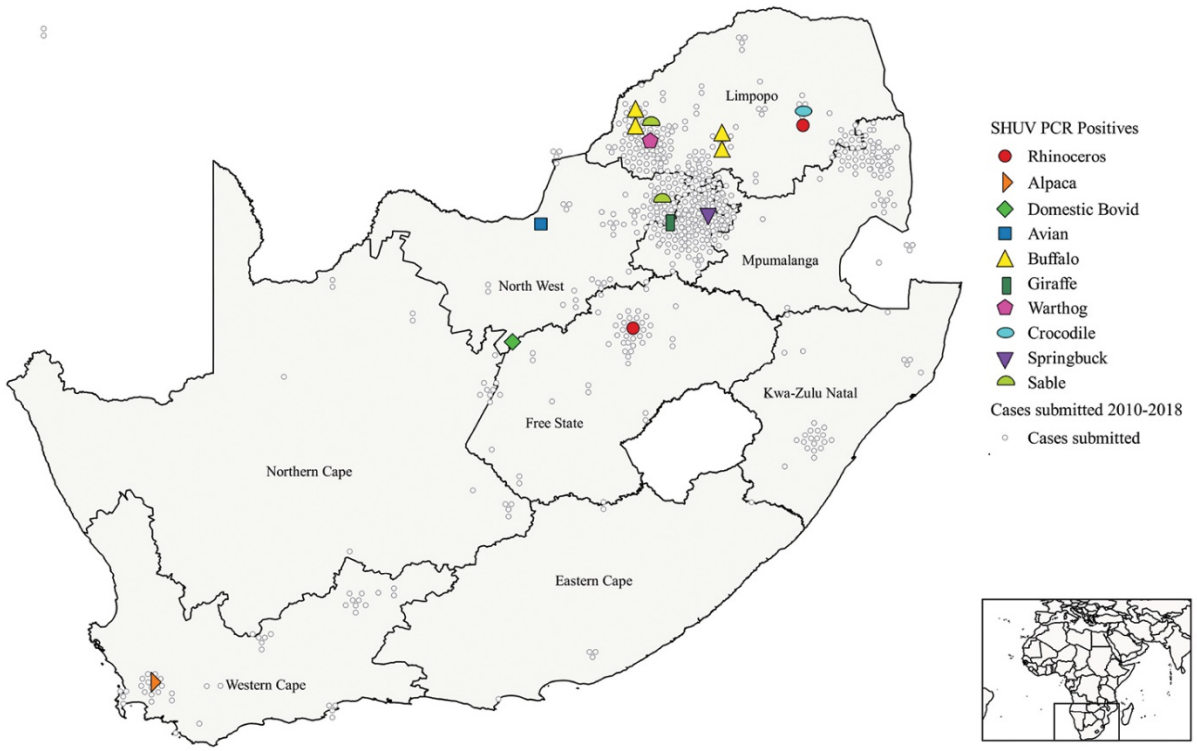

Appendix Figure 1. Map illustrating Shuni virus infections detected in wildlife, non-equine domestic animals and birds in South Africa from 2010 to 2018.

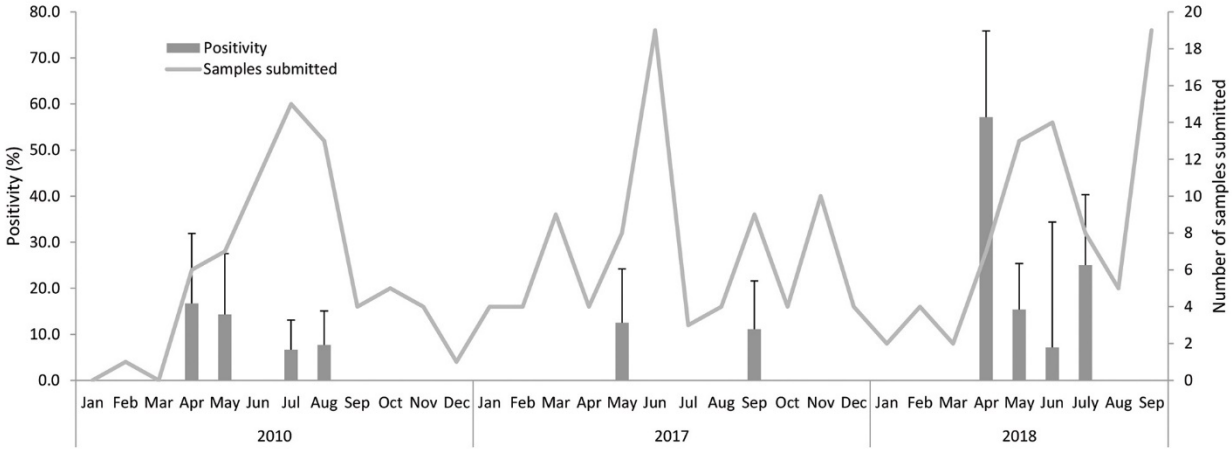

Appendix Figure 2. Seasonality of Shuni virus in wildlife and domestic animals during 2010–2018 in South Africa. Light gray bars indicate RT-PCR positives; line graph indicates samples submitted.

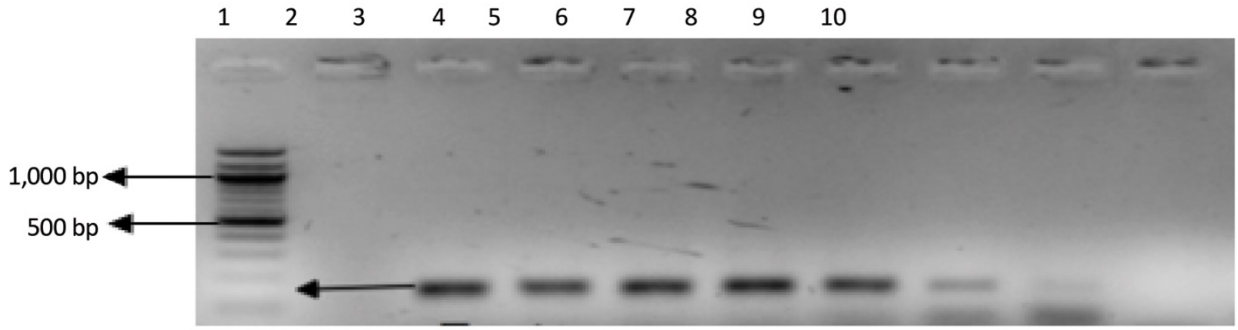

Appendix Figure 3. Agarose gel electrophoresis image showing Simbu/orthubunyavirus genus specific real-time TaqMan RT-PCR assay products separated on a 2.0% agarose gel. The band sizes were determined using a 100 bp molecular marker with an expected band size of 152 bp. Dilutions were made using the SHUV control (SAE18/09) and are displayed from the highest dilution (10^{0}) to the lowest (10^{-6}) (lanes 3–8) and a negative no-template control (lane 10).